

Development and incorporation of lightweight waste-based geopolymer aggregates in mortar and concrete

^aYliniemi, ^bPaiva, ^{b,c}Ferreira, ^dTiainen, ^{a*}Illikainen

^a Fiber and Particle Engineering Research Unit, P.O. Box 4300, 90014 University of Oulu, Finland

^b Civil Engineering Dept./CICECO, University of Aveiro, 3810-193 Aveiro, Portugal

^c Civil Engineering Dept./RISCO, University of Aveiro, 3810-193 Aveiro, Portugal

^d Laboratory of Inorganic Chemistry, Center for Molecular Materials, P.O. Box 3000, 90014, University of Oulu, Finland

*Corresponding author

mirja.illikainen@oulu.fi

Phone: +358405885904

P. O. Box 4300, FIN-90014, University of Oulu, Finland

Highlights

- Lightweight geopolymer aggregates were manufactured from fly ash and mine tailings
- Geopolymer aggregates have similar or better physical properties than LECAs
- Rheology of the mortar paste is similar for LECAs and geopolymer aggregates
- Geopolymer aggregates produced higher-strength mortars and concretes than LECAs

Abstract

Using industrial side streams as artificial aggregate precursors could increase waste utilization and save natural reserves. In this study, lightweight geopolymer aggregates were manufactured from fluidized bed combustion fly ash and mine tailings using high shear granulation and alkali activation. The results showed that geopolymer aggregates had physical properties comparable to commercial lightweight expanded clay aggregates (LECAs). Mortar and concrete prepared with geopolymer aggregates had higher mechanical strength, a higher dynamic modulus of elasticity, and higher density than concrete produced with LECAs, while the rheology and workability was the same.

Keywords: lightweight aggregates, rheology, geopolymers, mortar, concrete.

1. Introduction

The usage of lightweight aggregates (LWAs) in concrete is steadily increasing, as some of their properties, including reduced dead weight, higher insulating coefficients, and superior sound-dampening qualities, are better than those of normal-weight aggregates [1].

Natural LWAs, such as pumice, scoria, and tuff, have long been used as concrete aggregates [2]. However, with the increasing demand and non-availability of natural LWAs, methods for producing artificial LWAs have been developed. The most common artificial LWAs are lightweight expanded clay aggregates (LECAs), which are produced by expanding natural clay at about 1200 °C in rotary kilns. To save natural raw materials, prevent damaging mining activities, and increase waste utilization, there has been a great deal of research on manufacturing artificial LWAs from industrial side streams. The most common methods for producing artificial LWAs

from industrial waste are high-temperature sintering [3–7] and cement-based pelletization [8–12]. Another much less studied method is the granulation of wastes using alkali activators [13–15]. This method (i.e., geopolymerization) is economically sound, as it avoids the high costs of sintering and using cement. During the granulation, the surfaces of the precursor particles are wetted by the alkali activator. The reactive material dissolves and forms an alumino-silicate gel, which binds the particles together. The process results in spherical granules and surface dry granules.

Previous studies [15–17] have shown that geopolymer LWAs with satisfactory physical properties can be produced, even from low-reactivity and heavy metals containing fly ash. However, it is not clear how such aggregates perform in real mortar and concrete. As geopolymer aggregates may have different densities and levels of water absorption, the rheology (i.e., workability) of the cement mixture may change depending on the aggregates used. The intrinsic properties of LWAs also affect the properties of hardened mortar and concrete, such as their mechanical strength and capillarity.

Artificial LWAs are produced from mine tailings and fly ash using alkali activation and high shear granulation. The physical and mechanical properties of geopolymer aggregates are compared with commercial LECAs. Mortars and concretes are produced with LECAs and geopolymer aggregates and the rheology, mechanical strength, dynamic modulus of elasticity, capillarity, and density are determined. The aim of the research is to evaluate the performance of geopolymer aggregates in mortars and concretes.

2. Materials and methods

2.1 Materials

Two fluidized bed combustion (FBC) fly ashes and two mine tailings were chosen as geopolymer aggregate precursors. Fly ash 1 and fly ash 2 came from an electricity and heat power plant that uses wood and peat as fuel. Mine tailing 1 was obtained from a gold mine, and mine tailing 2 was obtained from a copper and zinc mine. The chemical composition of the raw materials is presented in Table 1.

Table 1. Chemical composition, loss on ignition, and average particle size of the geopolymer aggregate raw materials.

	Fly ash 1	Fly ash 2	Mine tailing 1	Mine tailing 2
CaO, XRF [%]	16.2	13.8	11.7	10.9
SiO ₂ , XRF [%]	42.4	40.2	49.8	25.3
Al ₂ O ₃ , XRF [%]	9.4	10.1	10.7	7.0
Fe ₂ O ₃ , XRF [%]	14.8	22.3	9.1	25.7
Na ₂ O, XRF [%]	1.7	1.3	3.1	-
K ₂ O, XRF [%]	3.6	2.5	1.3	0.8
MgO, XRF [%]	3.7	2.8	6.7	6.6
P ₂ O ₅ , XRF [%]	3.7	3.3	0.2	0.1
TiO ₂ , XRF [%]	0.3	0.3	1.3	0.4
SO ₃ , XRF [%]	3.2	2.4	4	13.6
Cl, XRF [%]	0.2	0.1	0	0.0

Moisture [%]	0.1	0	0.2	0.3
Loss on ignition 525°C [%]	0.1	0.1	0.2	1.6
Loss on ignition 950°C [%]	1.0	0.5	13.6	8.8
Particle median size <50% [μm]	14.7	20.7	130.4	126.1

77

78 The raw materials were granulated using a high-shear granulator (Eirich R01) and a sodium silicate
79 solution as an alkali activator. The geopolymerization process is explained in detail in [15]. In
80 brief, the process was as follows: 1) dry raw materials were weighed, mixed, and added to the
81 drum; 2) the impeller and drum were switched on, and approximately 15 g of sodium silicate
82 solution was added to prevent dusting; and 3) sodium silicate was added by the drop until the
83 desired aggregate size (2–10 mm in diameter) was achieved. Each geopolymer aggregate batch
84 was sealed in airtight plastic bags and stored in ambient conditions for 28 days. The sodium silicate
85 solution used for granulation was Zeopol® 25 (Huber), which has a SiO₂/Na₂O-molar ratio of 2.5
86 and a water content of approximately 66 wt%.

87 The particle density and water absorption of the aggregates were determined according to the EN
88 1097-6 standard [18]. The loose bulk density and voids were determined according to the EN 1097-
89 3 standard [19]. The particle size distribution was determined according to the EN 933-1 standard
90 [20].

91 As reference materials, two sizes of LECAs were used. The LECA filler had a particle size
92 distribution of 0–3 mm, and LECAs 4–12.5 had a particle size distribution of 4–12.5 mm. For all
93 mortar and concrete samples, CEM II/B-L 32.5 N cement was used. Siliceous sand was used as an
94 additional aggregate in the mortar and concrete.

95

96 2.2 Preparation of mortars and concretes

97 Mortar and concrete samples were prepared by adding water, then cement and sand, and then
98 mixing them in a mixer for three minutes. The aggregates and extra water (the water absorption
99 capacity of aggregates (%) multiplied by the mass of the aggregates) were added and mixed for
100 three more minutes. Suitable mortar and concrete mixtures were first prepared with LECAs, and
101 then the aggregates were replaced according to their loose bulk volume rather than their mass, due
102 to the variations in their loose bulk densities. Aggregates were not pre-wetted prior to their addition
103 so that water-cement-paste would impregnate them and thus would enhance the interfacial
104 transition zone (ITZ.) It has been reported [21] that the water absorption rate of aggregates is
105 greatly reduced after the first 2–5 min and that the absorption of pre-wetted aggregates after mixing
106 is not significant and only slightly affects the workability of fresh concrete. In this work, the water
107 addition was determined by measuring the water absorption capacity after 24 hours of immersion
108 in water. Thus, the amount of extra water was probably slightly higher than what was necessary.

109 For mortar samples, the aggregates were 0–2 mm in diameter (Figure 1), and for concrete samples,
110 they were 2–8 mm in diameter (Figure 2). For concrete samples, geopolymer aggregates had
111 different size distributions between the aggregate batches (Figure 2). To minimize the effect of the
112 aggregate size, two reference samples (C0a and C0b) were prepared by mixing the LECA filler
113 and LECAs 4–12.5 to obtain similar size distributions (LECA a and LECA b) as geopolymer
114 aggregates. The composition of each sample is presented in Table 2.

115

116

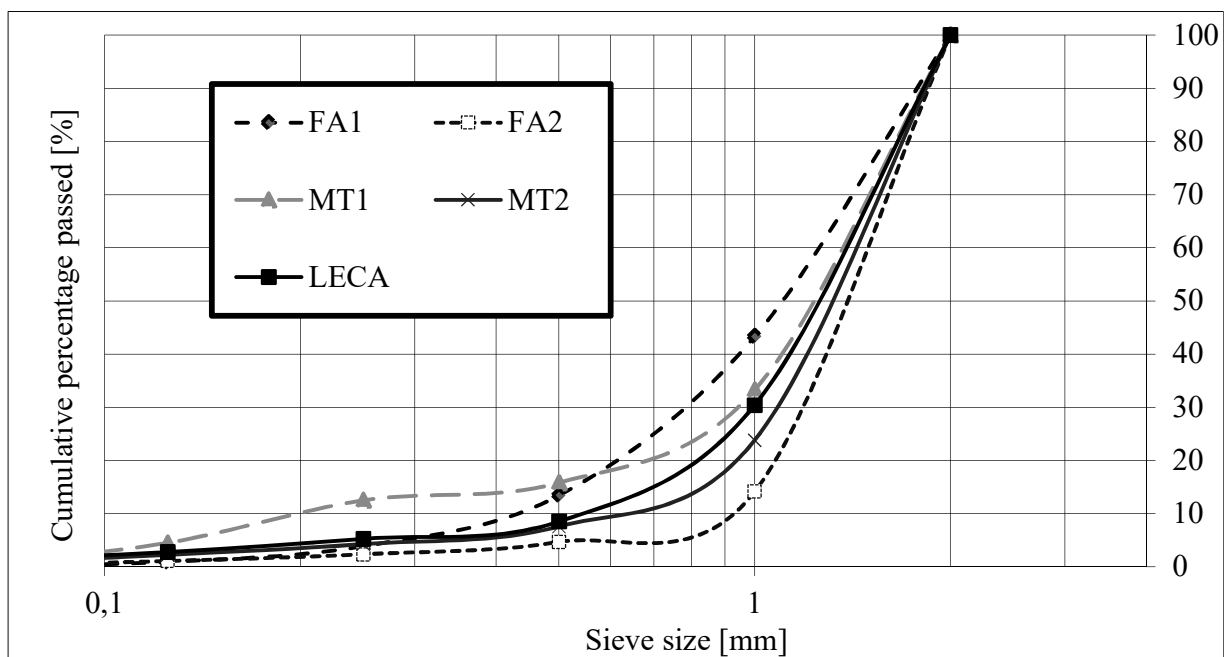


Figure 1. Aggregate size distributions for the mortar samples. FA: fly ash geopolymer aggregates; MT: mine tailing geopolymer aggregates.

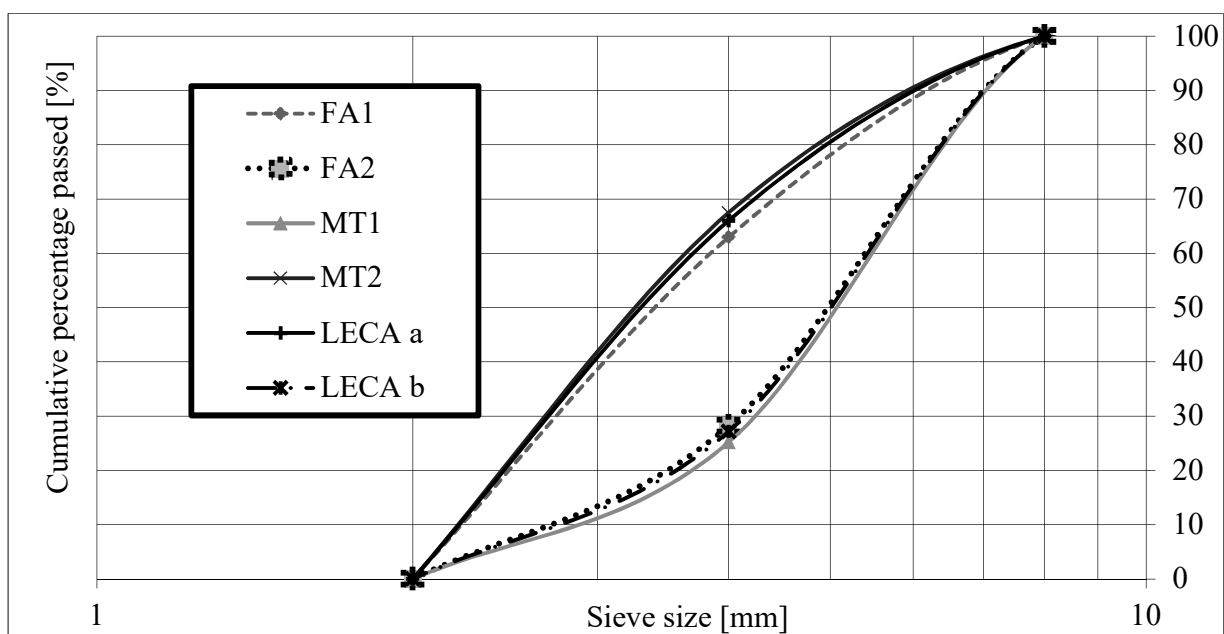


Figure 2. Aggregate size distributions for the concrete samples. FA: fly ash geopolymer aggregates; MT: mine tailing geopolymer aggregates.

Table 2. Composition of mortar and concrete samples. W/C = water/cement ratio of the paste mix. Additional water was added according to the water absorption and mass of the aggregates.

Mortar (aggregate size 0–2 mm)	Aggregate	Cement m-%	Sand m-%	Aggregate V-%	W/C (g/g)
M0	LECA	22	57	21	57
M1	FA1	22	57	21	57
M2	FA2	22	57	21	57
M3	MT1	22	57	21	57
M4	MT2	22	57	21	57
Concrete (aggregate size 2–8 mm)					
C0a	LECA a	22	59	19	63
C0b	LECA b	22	59	19	63
C1	FA1	22	59	19	63
C2	FA2	22	59	19	63
C3	MT1	22	59	19	63
C4	MT2	22	59	19	63

The mortar and concrete mixtures were cast into molds (4x4x16 cm³ molds for mortar samples and 10x10x10 cm³ molds for concrete samples). The mortar samples were hardened in a 20±5 °C and 65±5 % relative humidity (RH) room, while the concrete samples were cured at 95±5 % RH for 28 days at 20±5 °C.

2.3 Testing procedures

Additional mortar mixtures were prepared for the rheology measurements. Rheology behavior was determined using a Viskomat NT rheometer. Mortars usually behave as a Bingham fluid, characterized by yield stress and plastic viscosity. This apparatus automatically measures torque continuously during the test, following a speed–time program. Bingham behavior can be expressed as the relation between torque (T) and rotation speed (N): $T = g + h N$, where g and h are coefficients that are directly proportional to yield stress and plastic viscosity, respectively [22,23].

The method used to measure the rheological parameters was the profile of velocity versus time. The sample was mixed at 100 rpm during the test time (90 minutes) with a rotation reduction until 0 every 15 minutes (a ramp mode every 15 minutes).

The capillary water absorption of the hardened mortar samples was determined according to standard EN 1015-18 [24].

A field emission scanning electron microscope (FESEM, Zeiss Ultra Plus) was used to analyze cross-sections of the mortar samples. Pieces of the crushed samples were impregnated in an epoxy resin under a vacuum. After curing for 24 h, 2-mm slices were cut and placed in a plastic mold with a diameter of 40 mm. The slices were then impregnated in epoxy resin under a vacuum and left to cure for 24 h. The hardened samples were ground, polished, and coated with carbon to obtain an optimal surface for FESEM analysis. The distance between the sample and the beam tip was 5 mm. The acceleration voltage was 5 kV for secondary electron (SE) images and 15 kV for back-scattering electron (BSE) and energy dispersive x-ray spectrometer (EDS) images.

The forces required to crush the aggregates were measured with Shimadzu AG-IC testing machine by placing a single aggregate between two steel plates to its steadiest position, and the force needed to break the aggregate was measured. At least six aggregates were measured from each aggregate batch. The compression speed in the aggregate crushing test was 0.6 mm/min.

The mortar samples' flexural and compressive strength was measured using a testing machine (Shimadzu AG-IC) according to standard EN 1015-11:1999 [25]. The compressive strength of the concrete samples was determined using a test machine (FORM+TEST type Beta 2 3000D) according to the standard NP EN 12390-3:2009 [26]. The dynamic modulus of elasticity was measured using a portable ultrasonic nondestructive digital indicating test (PUNDIT).

3. Results and discussion

3.1 Physical properties of the aggregates

The loose bulk density was 1.0 g/cm³ for fly ash geopolymer aggregates and 0.9 g/cm³ for mine tailing geopolymer aggregates (Table 3). LECAs were much lighter, with a loose bulk density of only 0.4 g/cm³ for those that were 4–12.5 mm in diameter and 0.7 g/cm³ for those that were 0–3 mm in diameter. As expected, all aggregates were lightweight according to standard EN 13055-1 [27]. The water absorption of LECAs, FA1, and MT4 after 24 h was approximately 30 %. FA2 and MT1 displayed 21.5 % and 25.1 % water absorption, respectively.

Figure 3 shows the crushing forces of the aggregates. LECAs required a higher crushing force than the mine tailing geopolymer aggregates, but a lower crushing force than fly ash geopolymer aggregates. This indicates that there was more reactive material for the geopolymerization reaction in fly ash than in mine tailings. This was expected, as a previous study [28] using mine tailings as a geopolymer precursor showed that only low-strength materials can be obtained from mine tailing-only geopolymers.

Table 3. Physical properties of geopolymer aggregates and LECAs. Determinations were made according to standards 1097-3 and 1097-6.

	FA1	FA2	MT1	MT2	LECA 0–3	LECA 4–12.5
Apparent particle density (g/cm ³)	3.2	3.1	3.0	4.6	1.6	0.8
Oven-dried particle density (g/cm ³)	1.6	1.9	1.7	1.9	1.1	0.6
Wet-saturated particle density (g/cm ³)	2.1	2.3	2.1	2.5	1.4	0.8

Water absorption after 24 h (%)	30.7	21.5	25.1	31.3	29.9	32.6
Loose bulk density (g/cm ³)	1.0	1.0	0.9	0.9	0.7	0.4
Void volume (%)	36.1	46.4	46.6	51.2	37.2	36.5

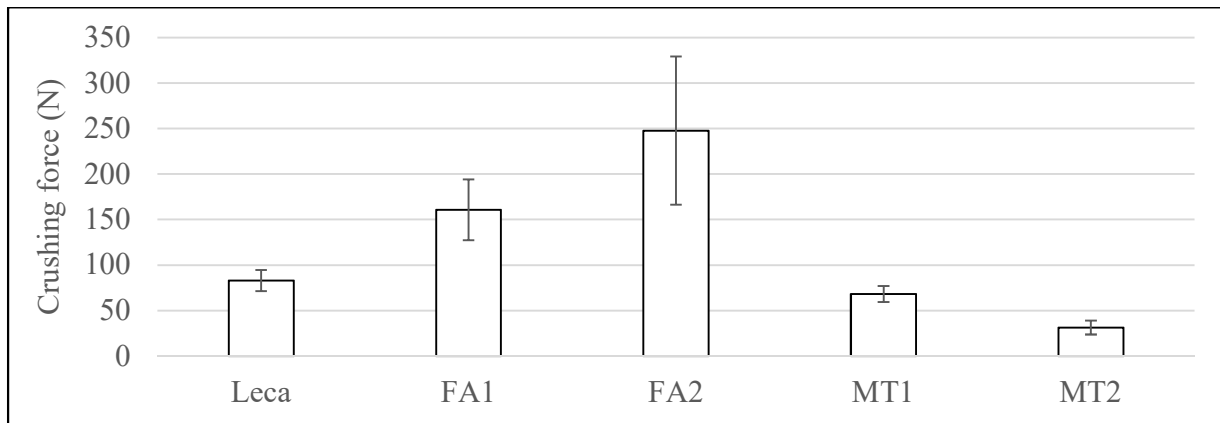


Figure 3. The forces required to crush the aggregates with a diameter of 5–7 mm. The error bars represent the intervals for the averages at a 95 % confidence level.

3.2 Mortar and concrete properties

Figures 4 and 5 present the plastic viscosity and yield stress, respectively, of the mortar samples based on the results of the rheology tests.

The parameter h , a coefficient proportional to plastic viscosity (Figure 4) decreased slightly during the first 15 minutes of the rheology measurement due to particle deagglomeration and the particles' orientation to the flow of the mortar. After 15 minutes of testing, the rheological parameters remained nearly unchanged until the end of the test, when workability was completely lost.

Figure 5 shows the behavior of the g parameter. For the first 15 minutes of the test, the g values decreased due to particle deagglomeration and particles' orientation to the flow. Afterwards, parameter g , the coefficient proportional to yield stress, increased steadily due to decreasing workability. M1 presents g values slightly lower and with the same trend than those observed for M0 and M4 compositions.

The rheological parameters of LECAs, FA, and MT geopolymer aggregates display similar behaviors. This is very important because if the rheological behavior of all compositions is identical, differences in the properties of hardened samples can only be due to the components of each composition.

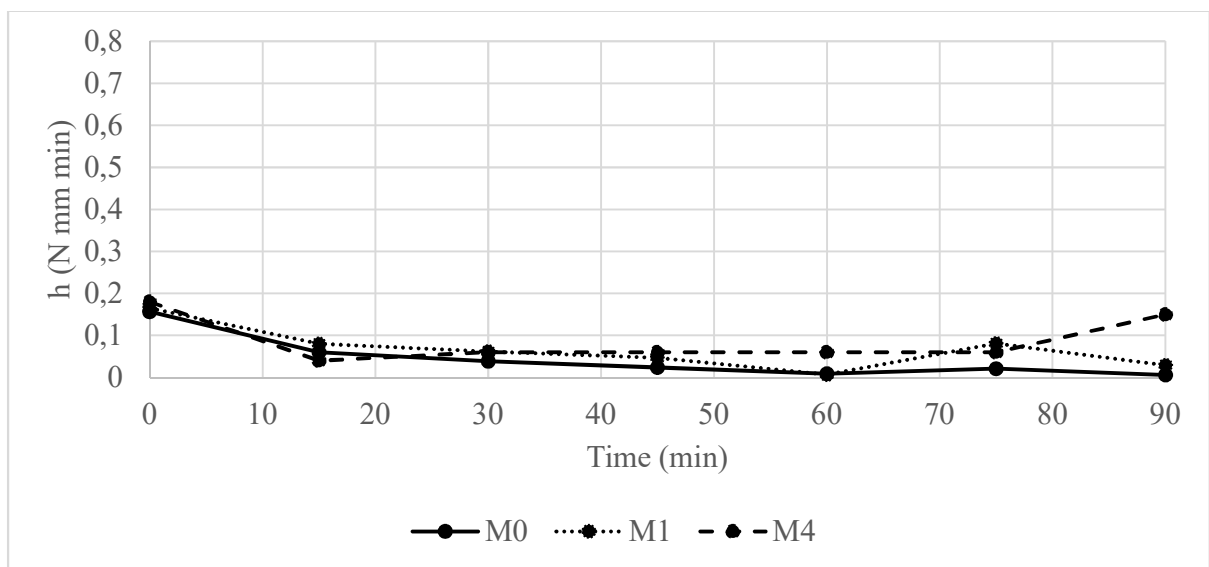


Figure 4. Variation in the h parameter during the test time of mortar samples

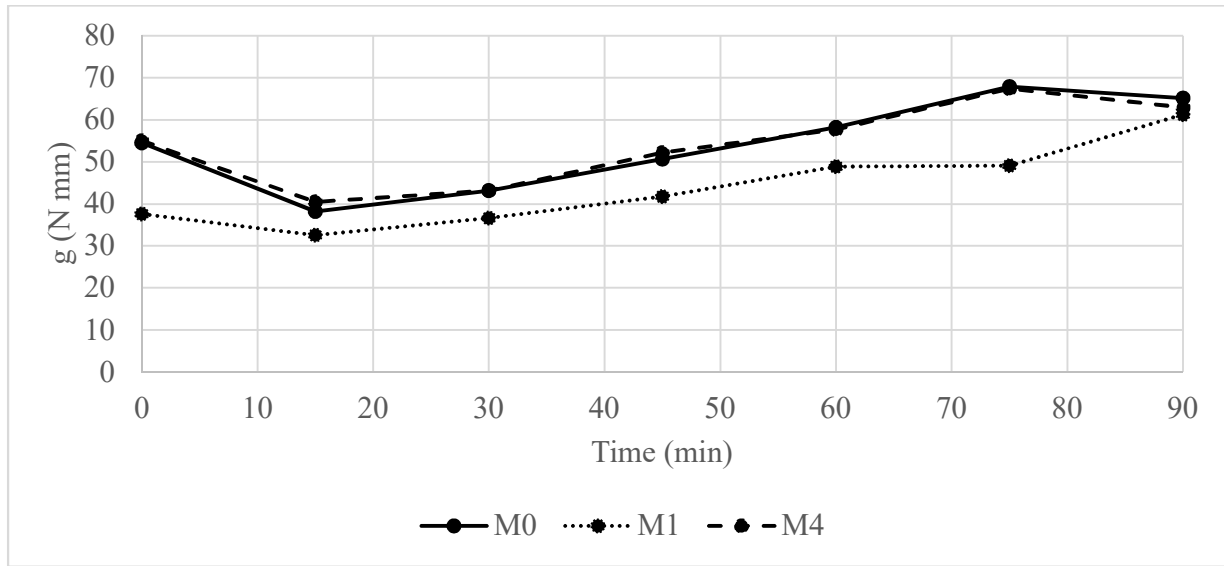


Figure 5. Variation in the g parameter during the test time of mortar samples.

Mortars prepared with geopolymer aggregates had higher compressive strengths than mortar with LECAs (Figure 6). Mortars with fly ash geopolymer aggregates gained compressive strength up to 26 MPa, while mortars produced with mine tailing geopolymer aggregates had a compressive strength of approximately 20 MPa. The flexural strength for all mortars was approximately 5 MPa, except for M2, which had slightly higher flexural strength (6.7 MPa). All geopolymer aggregate mortar samples had a higher dynamic modulus of elasticity compared to LECA mortar samples, showing higher stiffness (although the difference was only minor for M4). The dynamic modulus of elasticity may be also affected by the water content of the mortar [29], but this was not studied here.

The compressive strength of concrete samples behaved similarly to that of the mortar samples: FA geopolymer aggregates produced the strongest concrete, and LECAs produced the weakest (Figure 7). The actual compressive strengths of the concrete and mortar samples were also similar. This can be explained by the fact that LWAs are presumably the weakest components in the samples and therefore define their overall physical performance. The failure pattern of all samples was

satisfactory according to standard EN 12390-3 (type 1 in the standard). The fracture path travelled through the aggregates in all cases, showing that ITZ was stronger than aggregates.

The particle size distribution of the aggregates did not appear to have a great effect, as C0a and C0b had nearly the same compressive strength. The concrete samples' dynamic moduli of elasticity was similar to that of the mortar samples: concrete produced with LECAs was softer than that produced with geopolymer aggregates. However, the E-value of mine tailing aggregates was higher in the concrete samples than in the mortar samples.

It should be noted that the LECAs used in this study are probably not the most appropriate for structural concrete. The water absorption (Table 3) was high for LECAs, which is not common in LWAs used in structural lightweight concretes. Nevertheless, the water absorption of the geopolymer aggregates was also high, so in that sense the results are comparable.

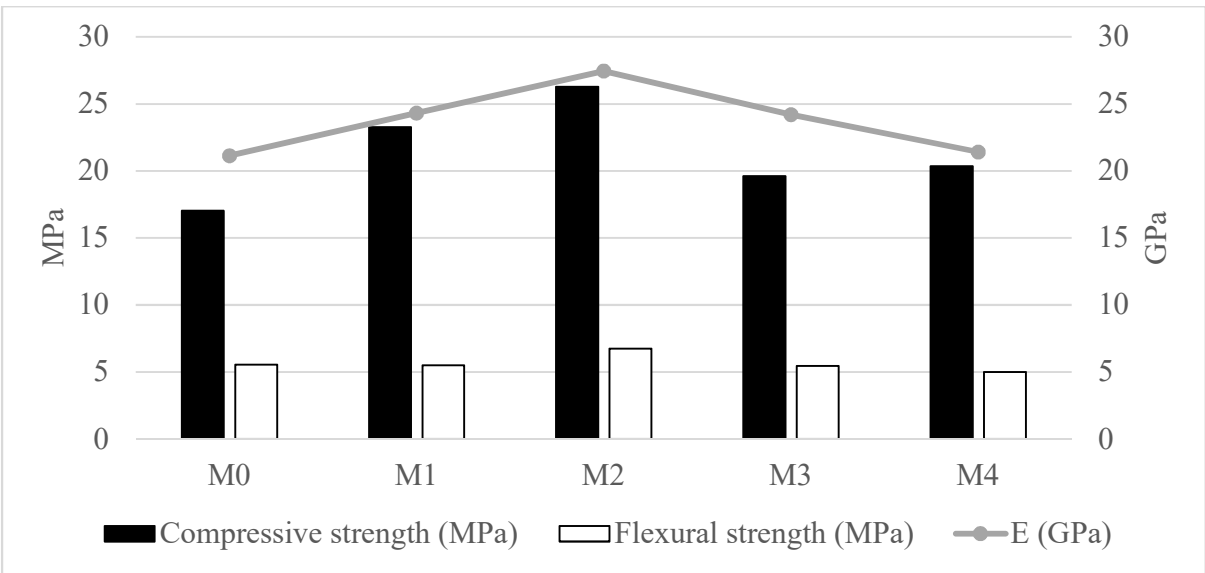
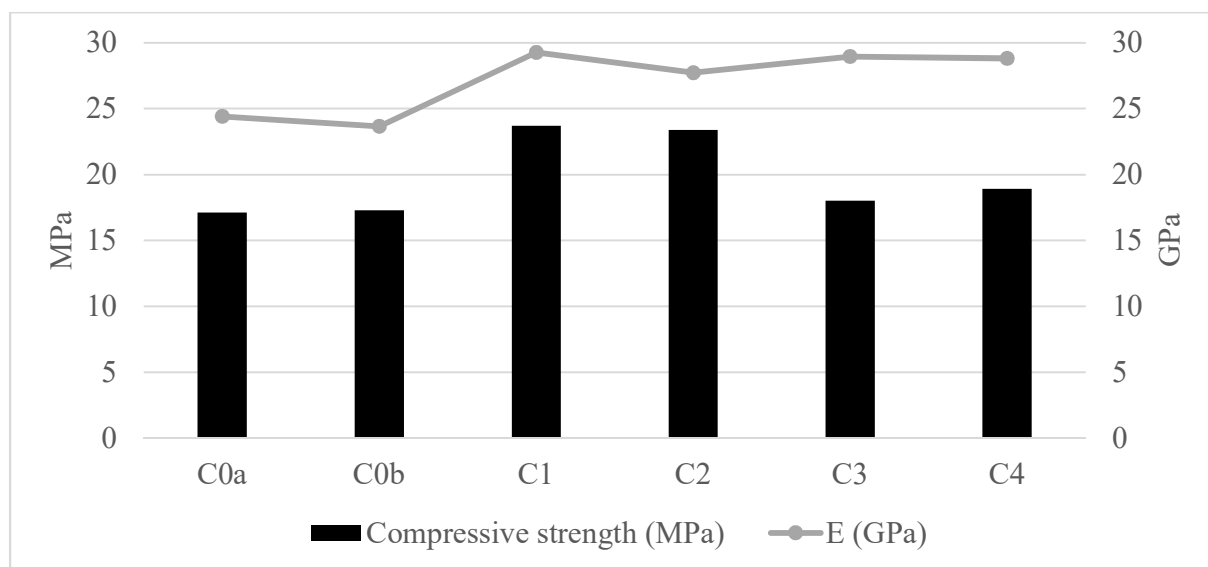


Figure 6. Compressive and flexural strengths of the mortar samples. The dynamic modulus of elasticity is shown as a line.

234



235

236 Figure 7. Compressive strength of the concrete samples. The dynamic modulus of elasticity is shown as a
 237 line.

238

239 The capillary water absorption of the mortar samples is presented in Figure 8. Mortar produced
 240 with LECAs absorbed more water more quickly than the geopolymer aggregate samples. M2 had
 241 the slowest water absorption, indicating that water is not able to penetrate FA2 aggregates as
 242 quickly as other aggregates. The total water absorption is shown in Table 4.

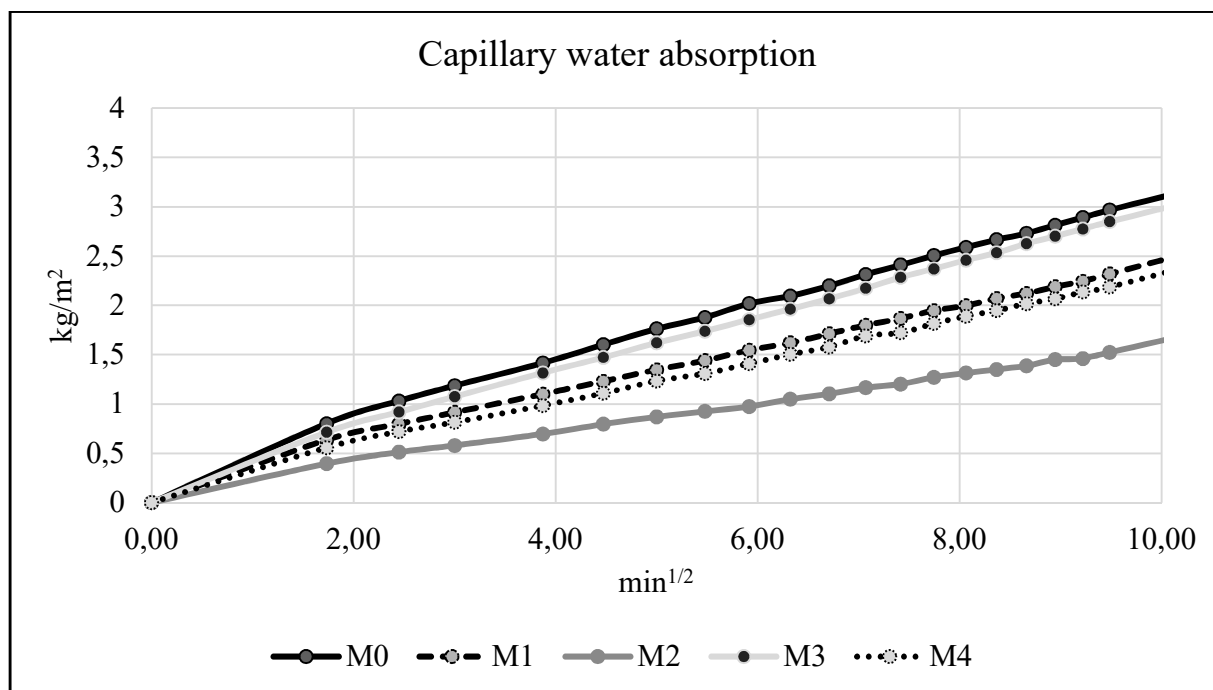


Figure 8. Capillary water absorption of mortar samples.

LECA mortar and concrete samples had an apparent density between 1730 and 1780 kg/m³ (Table 4). Geopolymer aggregate mortar samples had a higher apparent density (1900–1960 kg/m³), and geopolymer aggregate concrete samples had a density of about 2030 kg/m³ regardless of the aggregate used. Standard ASTM C567 states that structural lightweight concretes must have a maximum air-dry density of 1920 kg/m³. Geopolymer-based concretes did not achieve this density. However, the density of the samples was measured immediately after they were taken out of the curing chamber, meaning that they still had a high water content, which increased their weight. The densities of the mortar and concrete samples could be reduced by decreasing the amount of sand in the mixtures, as it is the main (and heaviest) component.

The total water absorption, shown in Table 4, was determined by conducting a capillary water absorption test for 90 min and immersing the sample under water for 24 h. After immersion, the

mortars were surface-dried and weighed. The total water absorption was around 10 % for all mortar samples except M2, which had a water absorption of only 7.9 %. Thus, M2 not only absorbed water slower than the other mortar samples but also absorbed less water than the other samples.

Table 4. Apparent density and total water absorption of the mortar and concrete samples.

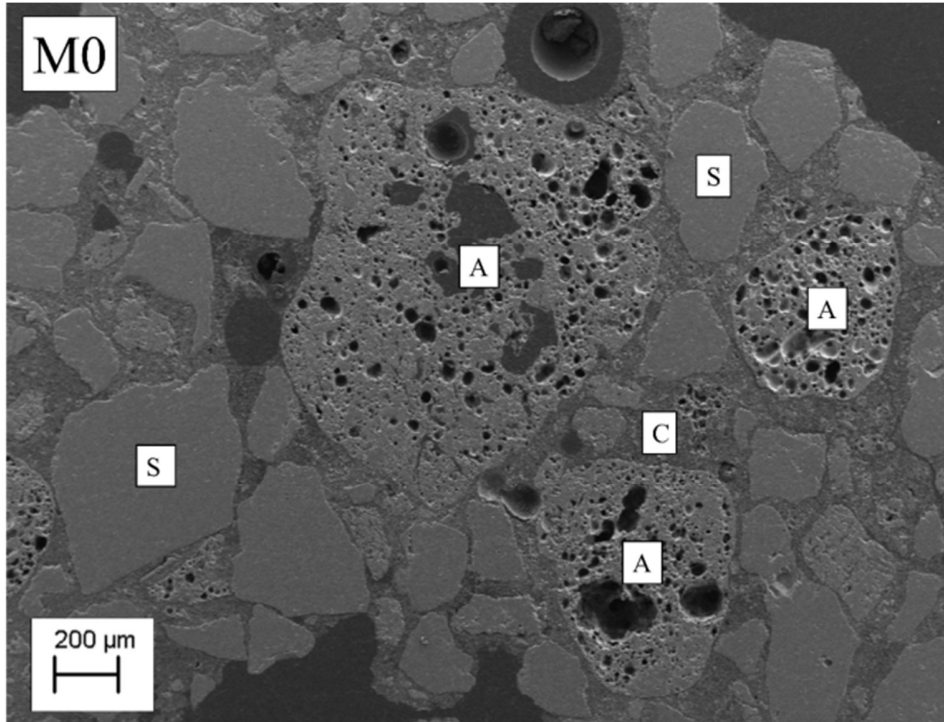
	Apparent density (kg/m ³)	Total water absorption [%]
M0	1731	10.2
M1	1907	10.1
M2	1943	7.9
M3	1907	9.9
M4	1959	9.6
C0a	1774	N/A
C0b	1763	N/A
C1	2025	N/A
C2	2029	N/A
C3	2033	N/A
C4	2023	N/A

3.3 Microstructure analysis

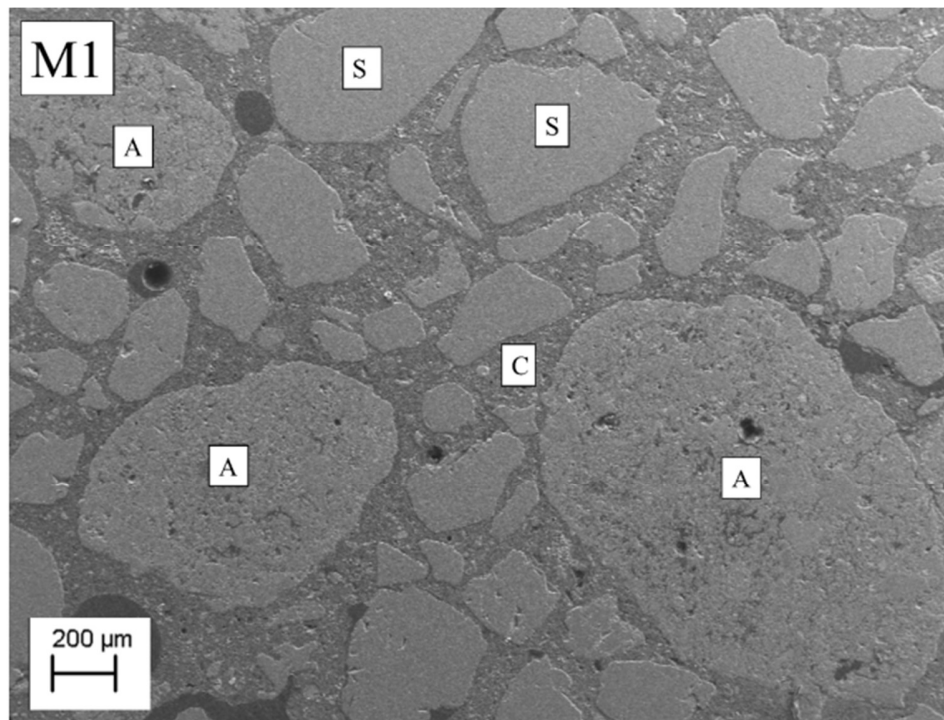
Figure 9 clearly shows the differences between the aggregates used to produce lightweight mortar. Sample M0 shows that LECAs are very porous, and large pores can also be observed in the cement matrix near the aggregate particles. This may have happened due to the coalescence of air inside the LECAs. These facts explain the low density, high capillarity, and low compressive strength of sample M0.

The LWAs in samples M1 and M2 are the densest aggregates in all the mortar samples. In addition, the cementitious matrix has low porosity and high density, and the mortar samples' microstructures have higher density and lower capillarity, leading to higher compressive strength.

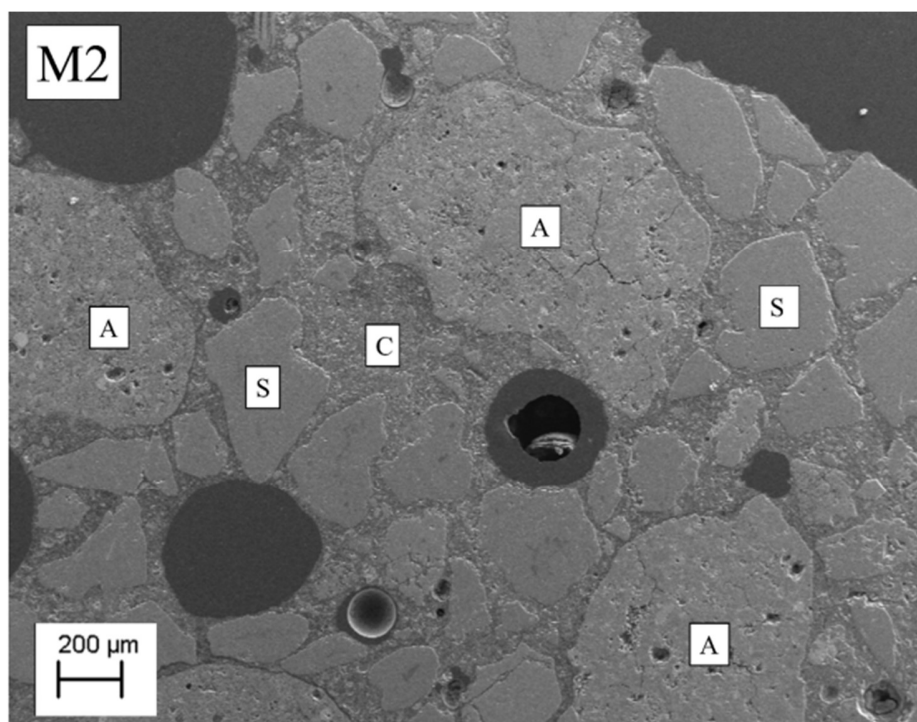
271 In samples M3 and M4, the pores of the aggregates are fragmented and connected to each other.
272 The MT mortar samples show a microstructure between the M0 mortar sample and the fly ash
273 LWA samples (M1 and M2).



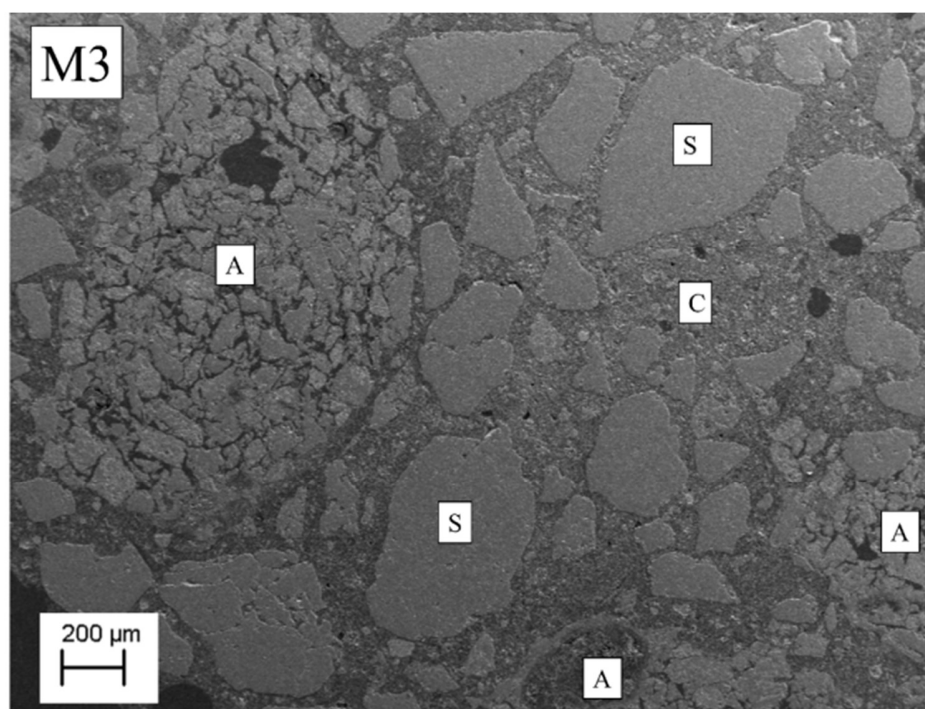
274



275



276



277

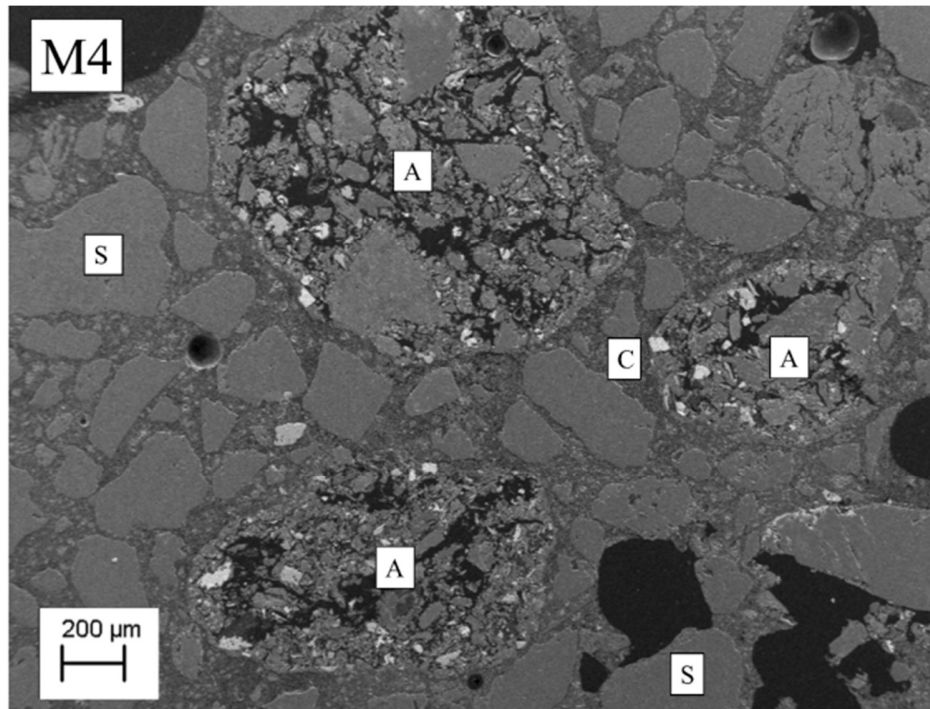


Figure 9. Secondary electron images of polished cross-sections of the mortar samples with LECAs (M0), fly ash (M1 and M2), and mine tailing (M3 and M4) geopolymer aggregates. A: aggregate; S: sand particle; C: cement binder.

Figure 10 shows a close-up view of the typical look of the cement–aggregate interface. LECAs and FA have smoother surfaces than MT aggregates. None of the mortar samples had a clearly visible porous ITZ. However, some gaps (tens of microns wide) were found between the FA aggregates and cement matrix in some parts of the samples (Figure 11). This seemed to be caused by the shrinkage of the FA aggregates. Surprisingly, MT aggregates seemed to expand, as there was a large number of pores inside the aggregates and tight binding to the cement matrix.

An EDS line analysis (data not shown) was conducted on multiple (6–10 spots/sample) aggregate–cement interfaces. Mortar samples that contained geopolymer aggregates had higher concentrations of Si and Na in the hydrated cement matrix near the aggregate surface. These elements originated from the aggregate binder (sodium silicate), which was the alkali activator

used in the granulation process. Other than that, no differences in the elemental composition of the samples' cement matrices were found.

4. Discussion

As aggregates were added according to their loose bulk density, the mortar and concrete samples had slightly different volumes of aggregates due to the difference in void volumes (Table 3). The difference between the highest void volume (MT2 51.2 %) and the lowest void volume (FA1 36.1 %) was 15.1 %, which means that mortar M4 had 3 % fewer aggregates (in volume of the total volume of the mixture) than mortar M1. Apparently, the difference in the aggregate volume did not have a significant impact on the physical properties of mortars and concretes, as the results were similar between LECAs, M1 & M2, and M3 & M4.

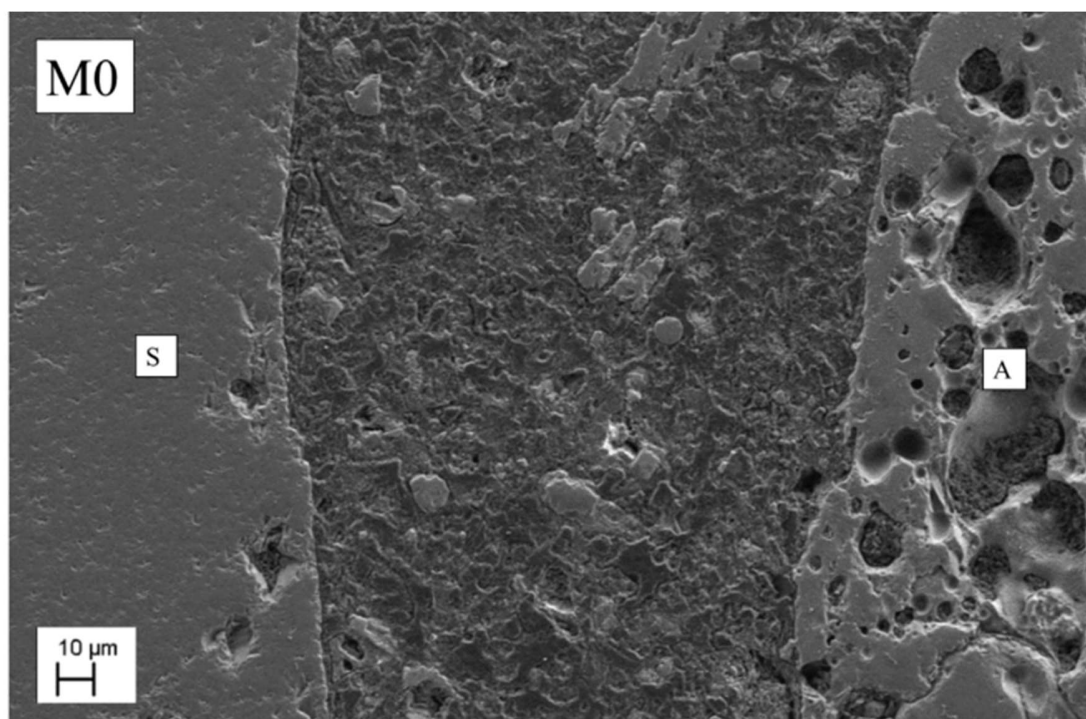
The purpose of not pre-wetting the aggregates prior to adding them to mortars was that water-cement-paste would go inside the aggregates when added (rather than water coming out of the aggregates) and would thus ensure proper binding between the aggregates and cement paste. As seen in microstructure analysis, indeed, the aggregates were well bound. However, as aggregates may absorb different amounts of water during mixing, the effective W/C-ratio may differ. A more detailed study to quantify the absorption of water in geopolymer aggregates during mixing would be valuable in future.

All the geopolymer aggregates produced higher compressive strengths than LECAs in mortar and concrete. This is logical for FA aggregates since LWAs are presumably the weakest part of the system and FA aggregates required higher crushing forces than LECAs. However, for MT aggregates, this was not the case; they were weaker than LECAs, but the compressive strength of the mortar and concrete samples was still higher. This indicates that an additional effect increased

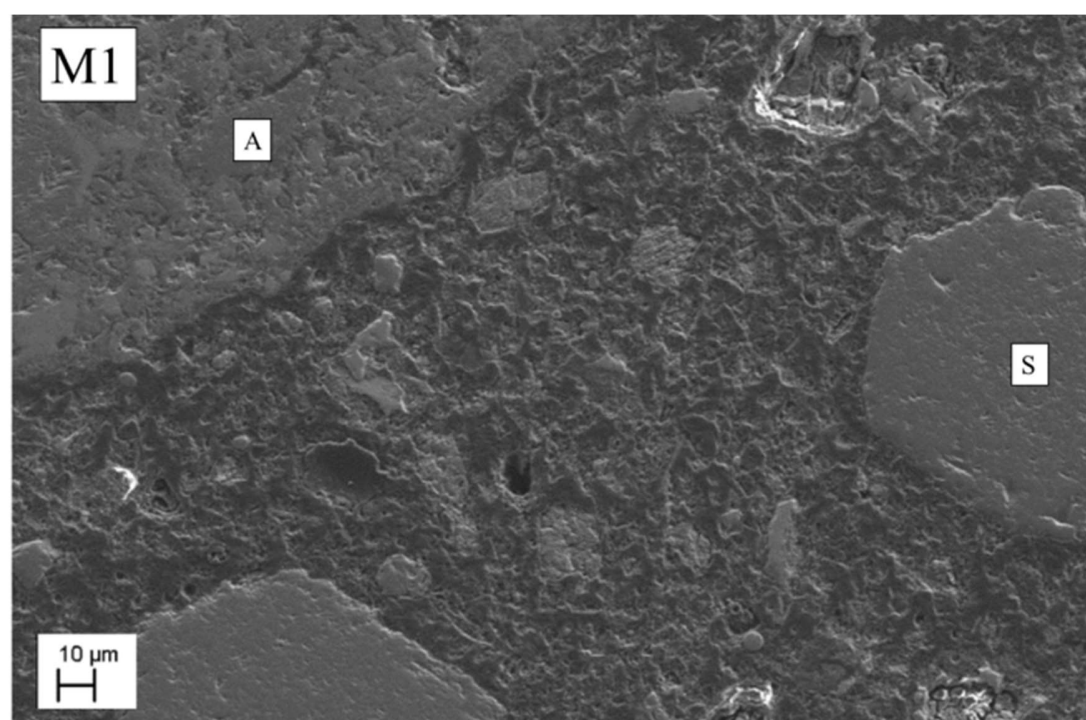
the samples' compressive strength when MT aggregates were used. One reason could be also the higher porosity of LECAs compared to MT aggregates (Table 3). Apparently, FA aggregates did not have the same effect, or at least not as extensively.

There were several other unexpected results that may be related to the physical or chemical properties of MT1 aggregates. The dynamic modulus of elasticity of C3 was similar to C1 and C2, while it had lower compressive strength. Additionally, M3 had higher capillary water absorption and total water absorption, although MT1 had low water absorption. Further studies with MT1 aggregates would be needed to resolve these findings.

A recent study by He *et al.* [30] concluded that the interfacial roughness of LWAs has a significant effect on the mechanical performance of mortar. The smoother outer layers of FA and LECAs could explain the lower-than-expected strength of FA and LECA aggregates and higher-than-expected strength of MT aggregates. Additionally, possible reactions [31] in the aggregate–cement interface could enhance the ITZ, thus increasing compressive strength more than could be predicted by the crushing force of the aggregates. Moreover, it should be determined whether alkali–silica reactions or salt leaching occurs over time.



329



330

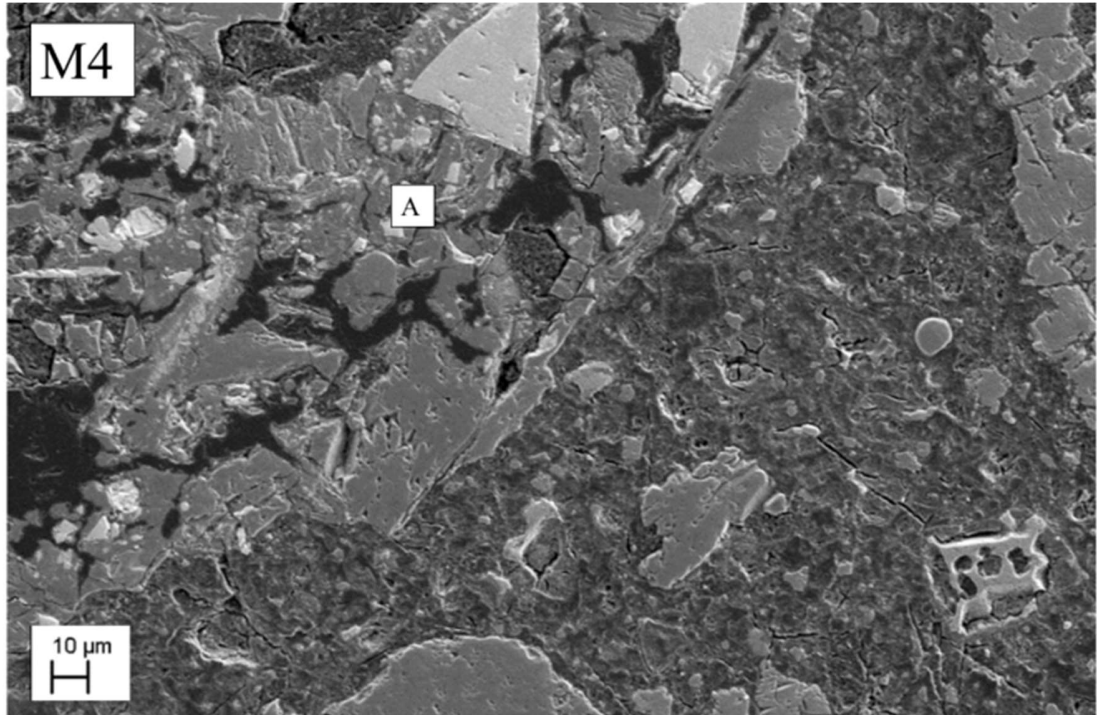


Figure 10. Secondary electron images of polished cross-sections of the mortar samples with LECAs (M0), fly ash (M1), and mine tailing (MT2) geopolymer aggregates. A: aggregate; S: sand particle. There was no clearly visible porous ITZ in any of the mortar samples.

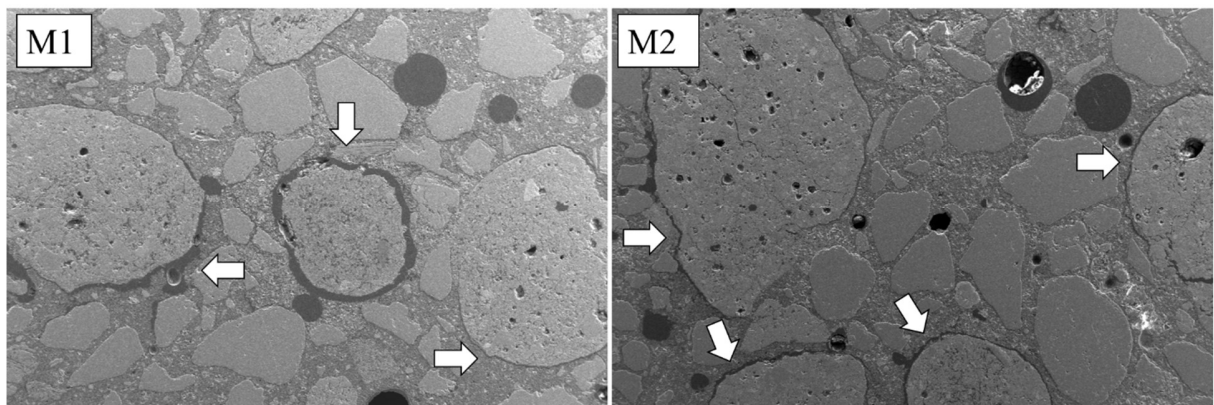


Figure 11. FESEM images showing the possible shrinkage of the FA aggregates.

5. Conclusions

Geopolymer aggregates produced from mine tailings and FBC fly ash were utilized as LWAs in mortars and concretes. The results of the study show that geopolymer aggregates produced better mechanical properties than LECAs in hardened mortar and concrete, while the rheology and workability of the fresh material is the same. The improved mechanical properties of fly ash geopolymer aggregates seem to be related to the higher required crushing force of the aggregates or better bonding due to the surface roughness of the aggregates. For mine tailing geopolymer aggregates the physical properties of mortars and concretes could not be explained by the aggregates' properties. Thus, further studies are needed. Nevertheless, the present study shows that there is potential in utilizing geopolymer aggregates in mortars and concretes.

Acknowledgements

This work was carried out as part of the GEOSULF ERA-MIN Project, which is supported by the Finnish Funding Agency for Technology and Innovation (Tekes), the Portuguese National Funding Agency for Science, Research and Technology (FCT), the National Center for Research and Development (BR), and various companies (Outotec, Agnico Eagle, and First Quantum Minerals). The authors would like to thank the Renlund Foundation for its financial support. Eng. Maria Carlos Figueiredo, Mr. Victor Rodrigues, Mr. Jarno Karvonen, Mrs. Elisa Wirkkala, and Mr. Jani Österlund are acknowledged for their contributions to the laboratory analyses. We also acknowledge the contributions of the personnel of the Center of Microscopy and Nanotechnology to the FESEM analyses.

362 **6. References**

- 363 [1] B. Jo, S. Park, J. Park, Properties of concrete made with alkali-activated fly ash lightweight
364 aggregate (AFLA), *Cem. Concr. Compos.* 29 (2007) 128–135.
- 365 [2] S. Chandra, L. Berntsson, *Lightweight Aggregate Concrete*, Noyes Publications, New
366 York, USA, 2002.
- 367 [3] B. González-Corrochano, J. Alonso-Azcárate, M. Rodas, J.F. Barrenechea, F.J. Luque,
368 Microstructure and mineralogy of lightweight aggregates manufactured from mining and
369 industrial wastes, *Constr. Build. Mater.* 25 (2011) 3591–3602.
370 doi:10.1016/j.conbuildmat.2011.03.053.
- 371 [4] B. González-Corrochano, J. Alonso-Azcárate, M. Rodas, F.J. Luque, J.F. Barrenechea,
372 Microstructure and mineralogy of lightweight aggregates produced from washing aggregate
373 sludge, fly ash and used motor oil, *Cem. Concr. Compos.* 32 (2010) 694–707.
374 doi:10.1016/j.cemconcomp.2010.07.014.
- 375 [5] V. Ducman, A. Mladenović, J.S. Šuput, Lightweight aggregate based on waste glass and its
376 alkali–silica reactivity, *Cem. Concr. Res.* 32 (2002) 223–226.
- 377 [6] C.-L. Hwang, L.A.-T. Bui, K.-L. Lin, C.-T. Lo, Manufacture and performance of
378 lightweight aggregate from municipal solid waste incinerator fly ash and reservoir sediment
379 for self-consolidating lightweight concrete, *Cem. Concr. Compos.* 34 (2012) 1159–1166.
380 doi:10.1016/j.cemconcomp.2012.07.004.
- 381 [7] O. Kayali, Fly ash lightweight aggregates in high performance concrete, *Constr. Build.*
382 *Mater.* 22 (2008) 2393–2399. doi:10.1016/j.conbuildmat.2007.09.001.
- 383 [8] M. Gesoğlu, E. Güneyisi, H.Ö. Öz, Properties of lightweight aggregates produced with
384 cold-bonding pelletization of fly ash and ground granulated blast furnace slag, *Mater.*
385 *Struct.* 45 (2012) 1535–1546. doi:10.1617/s11527-012-9855-9.
- 386 [9] H. Arslan, G. Baykal, Utilization of fly ash as engineering pellet aggregates, *Environ. Geol.*
387 50 (2006) 761–770. doi:10.1007/s00254-006-0248-7.
- 388 [10] C. Ferone, F. Colangelo, F. Messina, F. Iucolano, B. Liguori, R. Cioffi, Coal Combustion
389 Wastes Reuse in Low Energy Artificial Aggregates Manufacturing, *Materials.* 6 (2013)
390 5000–5015. doi:10.3390/ma6115000.
- 391 [11] R. Cioffi, F. Colangelo, F. Montagnaro, L. Santoro, Manufacture of artificial aggregate
392 using MSWI bottom ash, *Waste Manag.* 31 (2011) 281–288.
393 doi:10.1016/j.wasman.2010.05.020.
- 394 [12] F. Colangelo, F. Messina, R. Cioffi, Recycling of MSWI fly ash by means of cementitious
395 double step cold bonding pelletization: Technological assessment for the production of
396 lightweight artificial aggregates, *J. Hazard. Mater.* 299 (2015) 181–191.
397 doi:10.1016/j.jhazmat.2015.06.018.
- 398 [13] L.A. Bui, C. Hwang, C. Chen, K. Lin, M. Hsieh, Manufacture and performance of cold
399 bonded lightweight aggregate using alkaline activators for high performance concrete,
400 *Constr. Build. Mater.* 35 (2012) 1056–1062. doi:10.1016/j.conbuildmat.2012.04.032.
- 401 [14] F. Colangelo, R. Cioffi, Use of Cement Kiln Dust, Blast Furnace Slag and Marble Sludge in
402 the Manufacture of Sustainable Artificial Aggregates by Means of Cold Bonding
403 Pelletization, *Materials.* 6 (2013) 3139–3159. doi:10.3390/ma6083139.

- [15] J. Yliniemi, H. Nugteren, M. Illikainen, M. Tiainen, R. Weststrate, J. Niinimäki, Lightweight aggregates produced by granulation of peat-wood fly ash with alkali activator, *Int. J. Miner. Process.* 149 (2016) 42–49. doi:10.1016/j.minpro.2016.02.006.
- [16] J. Yliniemi, J. Pesonen, P. Tanskanen, O. Peltosaari, M. Tiainen, H. Nugteren, M. Illikainen, Microstructure and physical properties of lightweight aggregates produced by alkali activation-high shear granulation of FBC recovered fuel-biofuel fly ash, *Waste Biomass Valorization*. (2016).
- [17] J. Yliniemi, J. Pesonen, M. Tiainen, M. Illikainen, Alkali activation of recovered fuel-biofuel fly ash from fluidised-bed combustion: Stabilisation/solidification of heavy metals, *Waste Manag.* 43 (2015) 273–282. doi:10.1016/j.wasman.2015.05.019.
- [18] EN 1097-6, Tests for mechanical and physical properties of aggregates. Part 6: Determination of particle density and water absorption, 2014.
- [19] EN 1097-3, Tests for mechanical and physical properties of aggregates. Part 3: Determination of loose bulk density and voids, 1998.
- [20] EN 933-1, Tests for geometrical properties of aggregates. Determination of particle size distribution. Sieving method, 2000.
- [21] J.A. Bogas, A. Gomes, M.G. Gomes, Estimation of water absorbed by expanding clay aggregates during structural lightweight concrete production, *Mater. Struct.* 45 (2012) 1565–1576. doi:10.1617/s11527-012-9857-7.
- [22] P.F.G. Banfill, Rheology of fresh cement and concrete, *Rheol. Rev.* 2006 (2006) 61.
- [23] H. Paiva, L.M. Silva, J.A. Labrincha, V.M. Ferreira, Effects of a water-retaining agent on the rheological behaviour of a single-coat render mortar, *Cem. Concr. Res.* 36 (2006) 1257–1262. doi:10.1016/j.cemconres.2006.02.018.
- [24] EN 1015-18, Methods of test for mortar for masonry. Determination of water absorption coefficient due to capillary action of hardened mortar, 2002.
- [25] EN 1015-11, Methods of test for mortar for masonry. Determination of flexural and compressive strength of hardened mortar, 1999.
- [26] NP EN 12390-3, Testing hardened concrete. Part 3: Compressive strength of test specimens, 2009.
- [27] SFS EN 13055-1, Lightweight Aggregates for Concrete, Mortar and Grout, 2002.
- [28] J. Kiventerä, L. Golek, J. Yliniemi, V. Ferreira, J. Deja, M. Illikainen, Utilization of sulphidic tailings from gold mine as a raw material in geopolymerization, *Int. J. Miner. Process.* 149 (2016) 104–110. doi:10.1016/j.minpro.2016.02.012.
- [29] C.-C. Yang, Y.-S. Yang, R. Huang, The effect of aggregate volume ratio on the elastic modulus and compressive strength of lightweight concrete, *J. Mar. Sci. Technol.* 5 (1997) 31–38.
- [30] Y. He, X. Zhang, Y. Zhang, Y. Zhou, Effects of particle characteristics of lightweight aggregate on mechanical properties of lightweight aggregate concrete, *Constr. Build. Mater.* 72 (2014) 270–282. doi:10.1016/j.conbuildmat.2014.07.043.
- [31] L. Kong, L. Hou, Y. Du, Chemical reactivity of lightweight aggregate in cement paste, *Constr. Build. Mater.* 64 (2014) 22–27. doi:10.1016/j.conbuildmat.2014.04.024.

